Journal of Cellular Biochemistry 84:12–26 (2002)

ARTICLES

Cloning and Characterization of Osteoactivin, A Novel cDNA Expressed in Osteoblasts

Fayez. F. Safadi,[1]* Jie Xu,[1] Steven L. Smock,[2] Mario C. Rico,[1] Thomas A. Owen,[2] and Steven N. Popoff[1]

[1]Department of Anatomy and Cell Biology, Temple University School of Medicine, Philadelphia, Pennsylvania 19140

[2]Department of Cardiovascular and Metabolic Diseases, Pfizer Global Research and Development—Groton Laboratories, Groton, Connecticut 06340

Abstract Osteoblast development is a complex process involving the expression of specific growth factors and regulatory proteins that control cell proliferation, differentiation, and maturation. In this study, we used the rat mutation, *osteopetrosis* (*op*), to examine differences in skeletal gene expression between mutant *op* and normal littermates. Total RNA isolated from long bone and calvaria was used as a template for mRNA differential display. One of many cDNAs that were selectively expressed in either normal or mutant bone was cloned and sequenced and found to share some homology to the human *nmb* and *Pmel 17* genes. This novel cDNA was named *osteoactivin*. Osteoactivin has an open reading frame of 1716 bp that encodes a protein of 572 amino acids with a predicted molecular weight of 63.8 kD. Protein sequence analysis revealed the presence of a signal peptide and a cleavage site at position 23. The protein also has thirteen predicted *N*-linked glycosylation sites and a potential RGD integrin recognition site at position 556. Northern blot analysis confirmed that osteoactivin was 3- to 4-fold overexpressed in *op* versus normal bone. RT-PCR analysis showed that osteoactivin is most highly expressed in bone compared with any of the other non-osseous tissues examined. In situ hybridization analysis of osteoactivin in normal bone revealed that it is primarily expressed in osteoblasts actively engaged in bone matrix production and mineralization. In primary rat osteoblast cultures, osteoactivin showed a temporal pattern of expression being expressed at highest levels during the later stages of matrix maturation and mineralization and correlated with the expression of alkaline phosphatase and osteocalcin. Our findings show that osteoactivin expression in bone is osteoblast-specific and suggest that it may play an important role in osteoblast differentiation and matrix mineralization. Furthermore, osteoactivin overexpression in *op* mutant bone may be secondary to the uncoupling of bone resorption and formation resulting in abnormalities in osteoblast gene expression and function. J. Cell. Biochem. 84: 12–26, 2002.

Key words: osteoactivin; osteoblast differentiation; osteopetrosis

Bone is a very dynamic tissue that undergoes continuous modeling/remodeling. Because osteoblastic bone formation and osteoclastic bone resorption are antagonistic processes that proceed simultaneously, bone metabolism must be tightly regulated at all times. During the first two decades of life when the skeleton is growing, there must be a net increase in bone mass such that bone formation exceeds bone resorption. Once the skeleton has reached maturity, there must be a constant balance between formation and resorption to ensure that there is no net gain or loss of bone; this highly regulated balance is called coupling [Marks and Hermey, 1996]. When the rate of bone resorption exceeds that of bone formation there is a progressive loss of bone (osteopenia), and the resulting osteoporosis is associated with a variety of conditions such as aging, post-menopausal estrogen deficiency, inflammation, and chronic steroid treatment. In fact, uncoupling of formation and resorption is a common feature of most metabolic bone diseases [Marks and Hermey, 1996]. As bone loss progresses, the structural integrity of the skeleton is compromised resulting in an increased incidence of bone fractures. With an aging population, the exponential

Grant sponsor: Pfizer, Inc. (to S.N.P. and F.F.S.); Grant sponsor: Temple University School of Medicine (to Bone Research Enterprise Program).

*Correspondence to: Fayez. F. Safadi, Ph.D., Department of Anatomy and Cell Biology, Temple University School of Medicine, 3400 N. Broad Street, Philadelphia, PA 19140.
E-mail: fsafadi@astro.temple.edu

Received 5 June 2001; Accepted 3 July 2001

DOI 10.1002/jcb.1259

increase in the incidence of osteoporotic fractures has become a major health care issue and a significant cause of morbidity and mortality.

Osteoblasts are derived from mesenchymal stem cells and differentiate into pre-osteoblasts and then mature osteoblasts under the influence of genetic, local and systemic factors [Triffitt, 1996]. Our understanding of the role that these factors play in regulating osteoblast differentiation and function has dramatically increased in recent years. A number of different techniques such as differential display [Ryoo et al., 1997; Xu et al., 2000], subtractive hybridization [Petersen et al., 2000], and, most recently, gene array analysis [Beck et al., 2001] have led to the identification of novel factors that regulate bone cell development and function. Among these factors are OF45 [Petersen et al., 2000], connective tissue growth factor (CTGF) [Xu et al., 2000], the TGF-β superfamily members, lefty-1 [Seth et al., 2000], best-5 [Grewal et al., 2000] and PROM-1 [Ryoo et al., 1997], murine osteoclast inhibitory lectin (mOCIL) [Zhou et al., 2001], and RANK-L [Horowitz et al., 2001; Teitelbaum, 2000]. Some of these factors promote osteoblast differentiation and enhance osteogenesis while others are produced by osteoblasts and regulate osteoclast development and/or function. Identification of such factors has potential therapeutic application in cases where an increase in bone formation or a decrease in resorption would have a beneficial effect, either locally (as in fracture repair or localized osteopenia) or systemically (as in generalized osteopenia).

In this study, we used an animal model of osteopetrosis, the *osteopetrosis* (*op*) mutation in the rat, to examine differential gene expression in bone from normal and osteopetrotic animals resulting from the severe skeletal phenotype and abnormalities associated with skeletal development in *op* mutants [Marks and Popoff, 1989]. The mammalian osteopetroses are a heterogeneous group of congenital or experimentally-induced mutations characterized by a generalized increase in bone mass resulting from defective osteoclast-mediated bone resorption [Popoff and Schneider, 1996]. These mutations are pathogenetically heterogeneous since the point at which osteoclast development or activation is intercepted differs for each mutation [Popoff and Marks, 1995]. In some osteopetrotic mutations, the primary defect is intrinsic to cells of the osteoclast lineage while in others the defect is extrinsic to cells of the osteoclast lineage and involves cells within the bone microenvironment that regulate osteoclast development and/or activity.

In the *op* mutation, the primary defect appears to be intrinsic to osteoclasts since bone resorption can be restored following the transplantation of bone marrow in which the donor cell population contains normal osteoclast progenitors [Popoff et al., 1994]. In *op* mutant rats, abnormalities involving osteoblast gene expression [Shalhoub et al., 1991], mineral homeostasis [Hermey et al., 1995], immune function [Yamamoto et al., 1994], and the endocrine system [Safadi et al., 1999] have also been described. Using the technique of mRNA differential display, we identified a novel cDNA that is highly upregulated in *op* compared to normal bone. Subsequent cloning and sequencing of the full-length cDNA revealed a sequence with homology to the previously reported human *nmb* and *Pmel 17* cDNAs. In addition to being the first report of this cDNA in a species other than human, these studies also show that the mRNA is expressed by osteoblasts in bone. The temporal regulation of mRNA expression during osteoblast differentiation and analysis of the predicted amino acid sequence are consistent with a gene that has a functional role in bone. We propose the name osteoactivin for the protein encoded by this cDNA.

MATERIALS AND METHODS

Reagents

All chemicals were of molecular biology grade or higher and were purchased from Sigma (St. Louis, MO) unless otherwise stated. All cell culture media was purchased from Invitrogen (Life Technologies, Gaithersburg, MD).

Animals

An inbred colony of *osteopetrotic* (*op*) mutant rats, consisting of heterozygous breeders, is maintained at Temple University School of Medicine (Philadelphia, PA). Homozygous mutants (*op*) are distinguished from normal littermates (+/?) by radiographic analysis between 1 and 3 days after birth by the failure of the mutants to develop bone marrow cavities. Because the genotype of phenotypically normal rats cannot be distinguished, except by breeding

experiments, the normal littermates used in this study were of either heterozygous (+/*op*) or homozygous (+/+) normal genotype. All animals were maintained and used according to the principles in the NIH Guide for the Care and Use of Laboratory Animals [1985] and guidelines established by the IACUC of Temple University.

RNA Isolation

Total cellular RNA was isolated from calvaria and long bones (femurs and tibiae) harvested from 2-week-old *op* mutant rats and their normal littermates. Prior to freezing, the ends of the long bones were removed at the growth plate and bone marrow was flushed from the shafts of normal bones with saline at 4°C. Flushing of the bone marrow was only possible in normal rats because there were no marrow cavities in *op* mutants. Total RNA was prepared from pools of a minimum of six samples per phenotype and bone site (calvaria versus long bone). For osteoblast cultures, at the end of the culture period, medium was removed, the cell layer was rinsed, scraped into a 50 ml conical tube, centrifuged and supernatant was discarded. Bone samples and cell pellets were flash frozen in liquid nitrogen and stored at − 80°C. Total RNA from long bones, calvaria or osteoblasts was prepared as previously described [Thiede et al., 1994] with some modifications. Briefly, frozen samples were pulverized on dry ice (for long bones and calvaria only), and then homogenized in 5 M guanidinium isothiocyanate, 72 mM β-mercaptoethanol, and 0.5% sarkosyl. Homogenates were layered over a CsCl cushion (5.7 M CsCl and 30 mM NaAc), centrifuged at 100,000*g* overnight, and total RNA recovered by precipitation of the resulting pellets. Soft tissue RNA was isolated using TriZol (Invitrogen) according the manufacturer's protocol. RNA concentration was quantitated and its integrity was determined as described previously [Xu et al., 2000].

Differential Display of mRNA

RNA samples isolated from long bone or calvaria were treated with DNase I (Roche Molecular Biochemicals, Indianapolis, IN) to eliminate any potential contamination with genomic DNA. The basic principle of mRNA differential display (DD) was first described by Liang and Pardee [1992]. Briefly, 0.5 μg RNA from each sample (total of four independent samples, mutant and normal/calvaria and long bone) was reverse transcribed using each of 12 two-base-anchored oligo-dT primers provided in the Hieroglyph mRNA profile kits (Beckman Coulter Inc., Fullerton, CA) to subdivide the mRNA population. First strand cDNAs were amplified by the polymerase chain reaction (PCR) for 30 cycles using one of four upstream arbitrary primers (also provided in the kit) and the same anchoring primers used for first strand synthesis as described previously [Xu et al., 2000]. This resulted in 48 possible primer combinations for each kit (total of five kits) and each PCR amplification was run in duplicate from the same first-strand cDNA template. All amplified cDNAs were radiolabled with ^{33}P-dATP ([α-^{33}P]dATP, 2500 Ci/mmol, Amersham Pharmacia Biotech, Piscataway, NJ). The radiolabeled PCR products were electrophoresed on 4.5% denaturing polyacrylamide gels and dried using the Genomyx LR differential display apparatus (Beckman Coulter). Following autoradiography, bands were visually assessed and those representing differentially expressed cDNAs (exclusively expressed or highly overexpressed in one phenotype and confirmed in duplicate PCR amplifications) were excised from the gel. Each cDNA of interest was reamplified by PCR and used to probe a Northern blot to confirm its differential expression.

Cloning of Rat Osteoactivin cDNA

When the cDNA later determined to be osteoactivin was confirmed to be differentially expressed in Northern blot analysis, it was cloned into PCR-Script (Stratagene, LaJolla, CA), miniprep DNA was prepared, and plasmids with the appropriately sized inserts were sequenced using standard dideoxy methodologies. Gaps and ambiguities in the sequence were handled by direct sequencing of required regions using specific primers. Approximately 600 bp of sequence corresponding to the 3′ end of rat osteoactivin was obtained from the differential display clone. This fragment was used as a probe to screen a λgt11 rat kidney cDNA library (Clontech, Palo Alto, CA) by conventional means. A single clone was identified after three rounds of screening. The insert in this clone was amplified by PCR and subcloned into pCR2.1-TOPO (Invitrogen). The complete cDNA sequence of osteoactivin was obtained following transposon insertion (Primer Island; PE Applied Biosystems, Foster City, CA) and

sequence analysis revealed an open reading frame of 1,716 bp. The sequence of rat osteoactivin has been deposited in GenBank under accession number AF184983.

Northern Blot Analysis

Twenty micrograms of total RNA from *op* mutant and normal bone, calvaria, normal osteoblast cultures or soft tissues were electrophoresed on 1% formaldehyde-agarose gels and transferred to nylon membranes (Scheicher & Schuell, Keene, NH). The cDNA for osteoactivin was ^{32}P-labeled ([α-^{32}P]dCTP, 6,000 Ci/mmol) using Rediprime^{TM}II kit (Amersham Pharmacia Biotechnology). Blots were hybridized in Church's buffer (1 mM EDTA, 1 mM Na_2HPO_4 pH 7.2, 1% BSA, 7% SDS) overnight at 65°C. Blots were then autoradiographed, stripped and reprobed with an 18S rRNA probe used as a control to normalize for differences in loading and transfer.

RT-PCR Analysis

Two micrograms total RNA isolated from either long bone, calvaria, osteoblast cultures or soft tissues was reversed transcribed to cDNA at 42°C for 50 min in a volume of 20 μl containing the following components: 1 × first strand buffer (6 × 250 mM Tris, pH 8.3, 375 mM KCl and 15 mM $MgCl_2$) 0.5 mM dNTP mix; 10 mM dithiothreitol (DTT); 0.5 μg oligo(dT)$_{12-18}$ and 20 U Superscript II (RNase H-free reverse transcriptase, Invitrogen). The reaction was then terminated at 70°C for 15 min, and 1 U RNase H (Invitrogen) was added to the reaction mixture, followed by incubation at 37°C for 10 min to remove the RNA. One microliter aliquots of the generated cDNA was amplified in 50 μl of PCR reaction mixture containing 1 nM primer sets, 10 μl 10 × buffer D (for osteoactivin) or buffer N (for 18S) (Invitrogen) 10 nM dNTP mix, 1 μl DMSO, 1 μl Advantage polymerase mix (Clonetech). The primers for osteoactivin were (sense: 5′-CCAGAAGAATGACCGGAACTCG-3′ and anti-sense: 5′-CAGGCTTCCGTGGTAGTGG-3′). These primers were designed from the 5′ end of the protein coding region starting at a position 729 bp from the ATG start codon to position 1280. Primers for 18S were (sense: 5′-ACTTTCGATGGTAGTCGCCGTGC-3′ and anti-sense: 5′-ATCTGATCGTCTTCGAACCTCCGA-3′). PCR was performed using Perkin-Elmer GeneAmp PCR System 9600. PCR parameters for osteoactivin were: denaturation step at 94°C for 3 min, followed by 25 cycles of 94°C for 20 s, 62°C for 20 s and 68°C for 20 s; with final extension step at 68°C for 7 min. The expected osteoactivin PCR product was 552 bp. PCR parameters for 18S were: denaturation step at 94°C for 3 min, followed by 30 cycles of 94°C for 30 s, 65°C for 30 s and 68°C for 30 s; with final extension step at 72°C for 7 min. The expected 18S PCR product was 700 bp. The PCR products were analyzed by 1% agarose gel electrophoresis stained with ethidium bromide. A 100 bp ladder was used as a molecular weight marker (Invitrogen).

Synthesis of Osteoactivin RNA Riboprobe

Approximately 600 bp fragment of the 3′ end of rat osteoactivin was cloned into the PCR Script plasmid vector flanked by T7 and T3 promoters. Osteoactivin RNA sense and antisense riboprobes were synthesized in the presence of digoxygenin (DIG)-modified UTP using an in vitro transcription kit (Roche) according to the manufacturer's protocol.

In Situ Hybridization of Osteoactivin in Bone

Tibae or femurs from normal rats were harvested, fixed in 4% paraformaldehyde, decalcified, embedded, and sectioned. Sections were baked at 60°C for 1 h, cleared in xylene, rehydrated in 100, 75, 50, 25% ethanol in PBT (PBS, 0.1% Triton X-100), and rinsed in PBT three times for 10 min each. Sections were treated with Proteinase K (10 μg/ml) in PBT and incubated at 37°C for 15 min, then rinsed twice in PBT 5 min each. Sections were then refixed in 0.2% glutaraldehyde and 4% parafomaldehyde in PBT at room temperature for 10 min and then rinsed briefly in PBT. Sections were placed in a humidified chamber and prehybridized (50% formamide; 5 × SSC; 2% blocking powder supplied in the kit (Roche Laboratories); 1 mg/ml yeast RNA; 5 mM EDTA and 50 μg/ml heparin) for 4 h at 60°C. Sections were then hybridized (prehybridization solution and osteoactivin-riboprobe at 5 ng/ml) at 60°C overnight. The following day, sections were subjected to different washes; 100% solution-1 (50% formamide, 5 × SSC, 0.1% Triton and 0.5% CHAPS); 75% solution-1 in 2 × SSC; 50% solution-1 in 2 × SSC and 25% solution-1 in 2 × SSC. Sections were rewashed with 2 × SSC and 0.1% CHAPS twice for 30 min each at 65°C; 0.2 × SSC and 0.1% CHAPS twice for 30 min each at 65°C and twice

for 10 min each with TBT (0.05 M Tris (pH 7.5), 0.1% Triton, 150 mM NaCl) at room temperature. Sections were then blocked with 10% sheep serum, 2% BSA in TBT for 1 h at room temperature and incubated overnight at room temperature with anti-DIG antibody (1:500 dilution in 10% sheep serum, 2% BSA in TBT). Following antibody treatment, sections were washed as follows: three times for 30 min each in 0.1% BSA in TBT at room temperature, twice 30 min each in TBT, three times 10 min each in Genius buffer (Genius buffer; 100 mM NaCl, 100 mM Tris HCl, 50 mM $MgCl_2$ pH 9.5) and 0.1% Tween 20. Signal was developed using the color developing solution (45 μl NBT and 35 μl X-phosphate in 10 ml of Genius buffer); sections were covered and placed in the dark at room temperature for 15–30 min or until the color change was observed. Color signal was fixed with 4% paraformaldehyde in PBT overnight at 4°C and sections were mounted in PBS-glycerol and examined using a Nikon-Eclipse E800 light microscope.

Primary Osteoblast Cultures

Normal rat pups (1–4-day-old) were euthanized and a mid-line skin incision was made to expose the calvaria. The periosteum was removed and frontal and parietal bones were dissected. These pieces of calvarial bone were transferred to siliconized Ehrlenmeyer flasks containing 10 ml of trypsin/collagenase P solution (0.25% trypsin and 0.2% collagenase P in PBS) and placed in a 37°C shaker for 5 min. Supernatant was discarded following the first digestion. Supernatants from the second (15 min at 37°C) and third (25 min at 37°C) digestions were pooled into MEM (Hank's) containing 10% FBS and penicillin (5,000 U/ml) and streptomycin (5 mg/ml). Cells were washed twice in MEM (Earl's) supplemented with 10% FBS penicillin/streptomycin, filtered through a 200 μm metal screen filter, followed by filtration through an ether/ethanol treated filter. Cells were counted and viability determined by trypan blue exclusion. Cells were plated in 100-mm dishes at a density of 5×10^5 cells/dish in plating medium (MEM (Earl's) with 10% FBS and penicillin/streptomycin. On day 3 of the culture, cells were fed with plating medium supplemented with ascorbic acid (25 μg/ml). On day 7 and every 3 days thereafter, cells were fed with plating medium containing ascorbic acid (50 μg/ml) and β-glycerolphosphate (10 mM) to induce osteoblast differentiation and promote mineralization. Osteoblast differentiation was assessed by the formation of mineralized bone nodules assessed by von Kossa staining [Popoff et al., 2000].

RESULTS

Identification of Osteoactivin

Total cellular RNA obtained from normal or *op* mutant calvaria or long bone was used as a template for differential display analysis. Many differences in gene expression were observed between mutant and normal bone with a typical autoradiogram shown in Figure 1. For

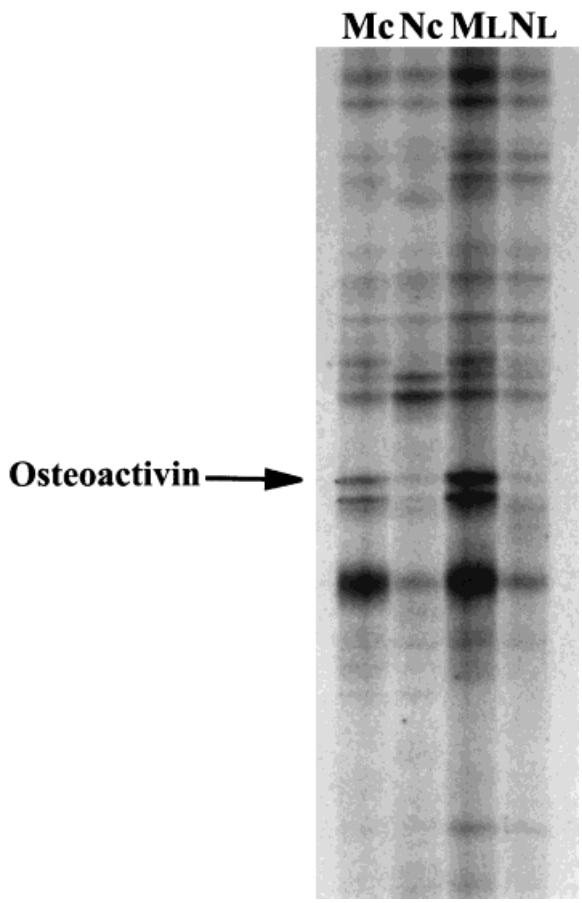

Fig. 1. Identification of osteoactivin using differential display analysis. Total cellular RNA obtained from mutant (M) or normal (N) calvaria (C) or long bone (L) was reversed transcribed using a two-base anchored oligo-dT primer (Hieroglyph mRNA profile kit). First strand cDNAs were used to generate radiolabeled PCR products using the same anchoring primer and an arbitrary upstream primer. Each PCR reaction was performed in duplicate and run on a denaturing acrylamide gel. The arrow indicates the band corresponding to osteoactivin and shows differential expression between mutant and normal bone samples.

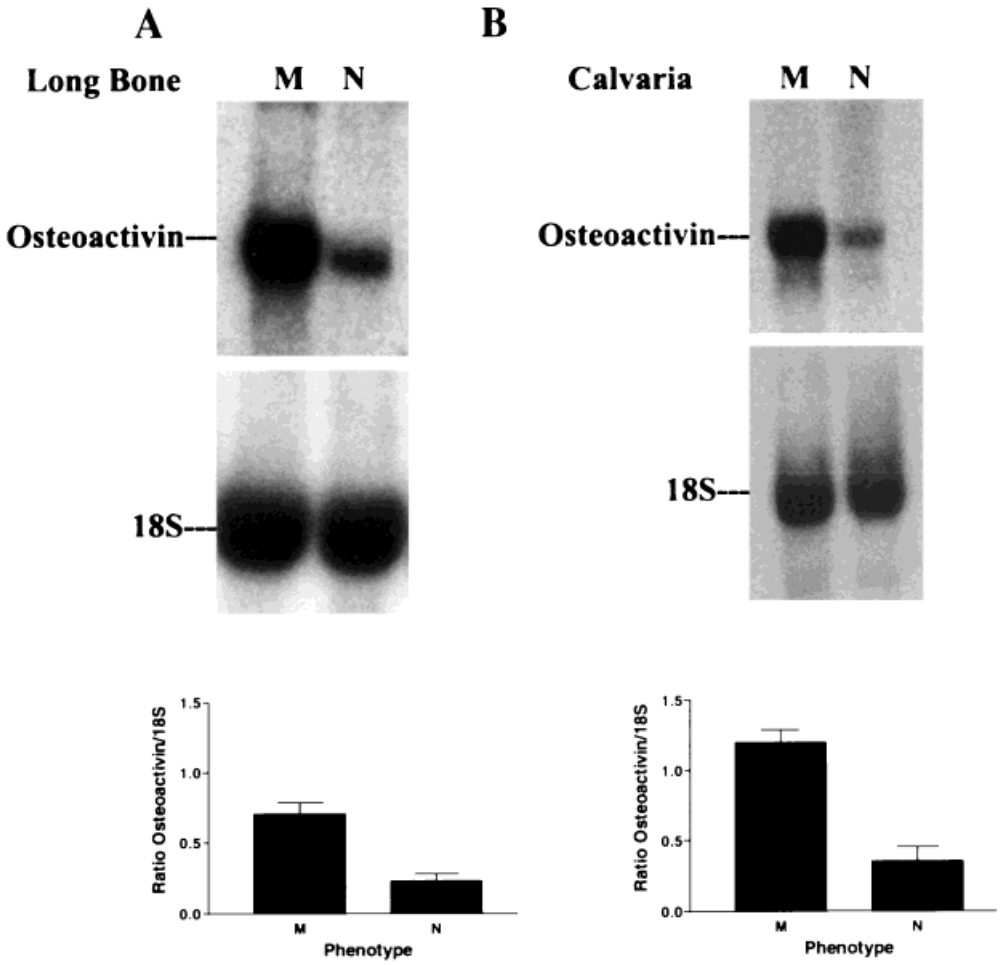

Fig. 2. Northern blot analysis of osteoactivin in bone. Representative Northern blots of osteoactivin expression in long bone (**A**) and calvaria (**B**) from *op* mutant and normal rats. Twenty micrograms of total RNA isolated from mutant (M) or normal (N) long bone (A) and calvaria (B) was electrophoresed in a 1% agarose-formaldehyde gel, blotted, and probed for osteoactivin. The blot was then stripped and reprobed for 18S rRNA as a control for gel loading. Northern analysis was repeated three times using independent RNA samples. Densitometric analysis showed the relative difference in osteoactivin expression in mutant when compared to normal bone.

osteoactivin, the upper of the two intense bands in mutant calvaria and long bone that is faintly visible in normal bone represents the band from which the original cDNA fragment was isolated (Fig. 1). This band was cut from the gel, DNA was extracted and used as a template for PCR reamplification. The resulting DNA was radiolabeled and used as a probe for Northern confirmation of differential expression of osteoactivin using RNA isolated from normal and mutant long bone and calvaria (Fig. 2). Densitometric analysis revealed that osteoactivin was highly (3- to 4-fold) overexpressed in *op* mutant compared with normal long bone (Fig. 2A) and calvaria (Fig. 2B).

Cloning and Characterization of Osteoactivin

The cDNA obtained from the differential display analysis was used as a probe to screen a λgt11 rat kidney cDNA library in an effort to obtain a full-length clone of osteoactivin. Approximately 10^6 clones were screened and one positive was obtained. This clone was completely sequenced and the sequence has been deposited in GenBank under accession number AF184983. The cloned rat osteoactivin has an open reading frame of 1,716 bp with 114 bp of 5′ untranslated sequence and 476 bp of 3′ untranslated sequence prior to the poly-A tail (data not shown). The open reading frame encodes a

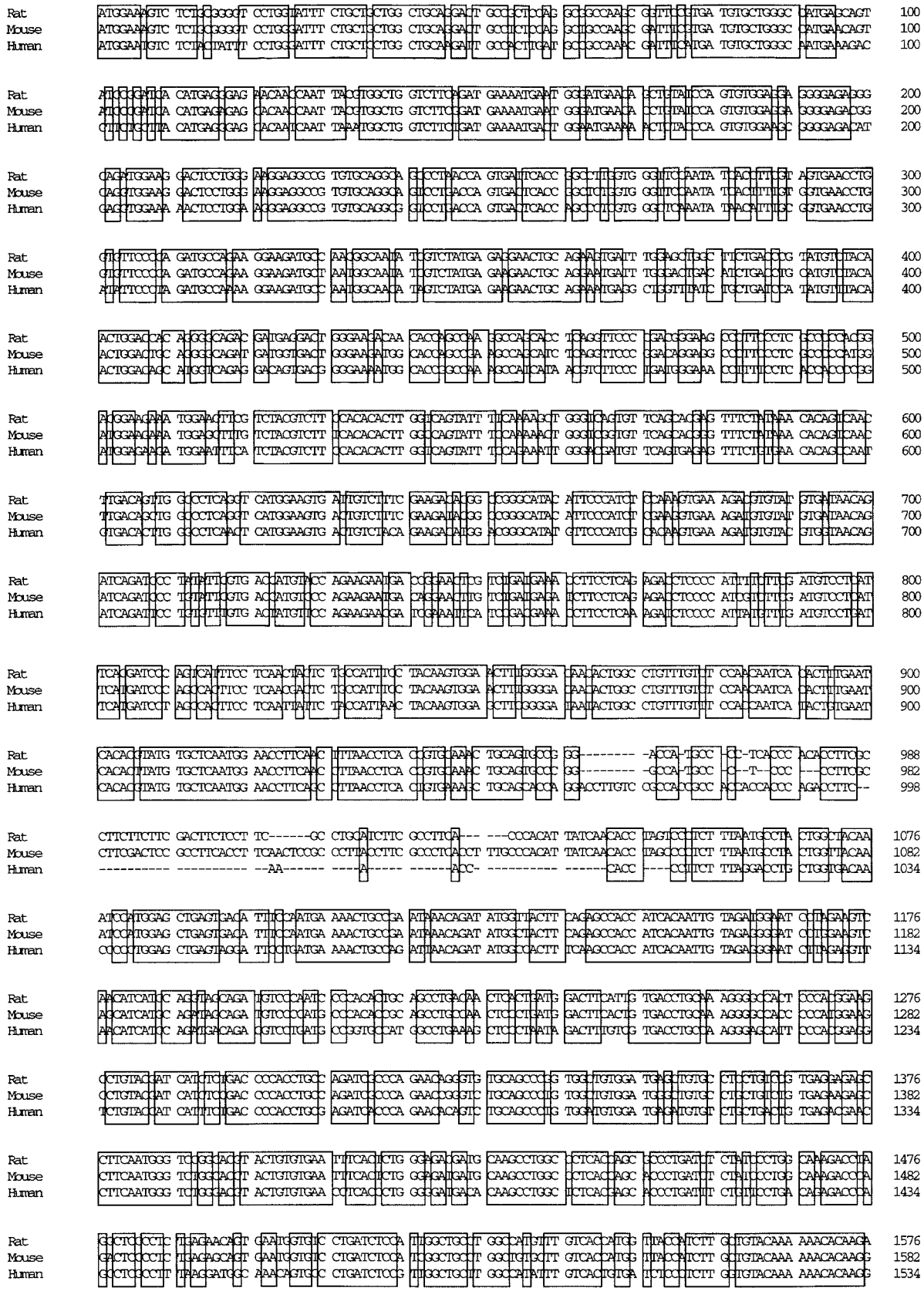

Fig. 3. Nucleotide sequence of rat osteoactivin open reading frame. The nucleotide sequence of rat osteoactivin is shown in comparison to mouse and human *nmb*. The open reading frame potentially encodes a protein of 572 amino acids with a predicted molecular weight of 63.8 kD.

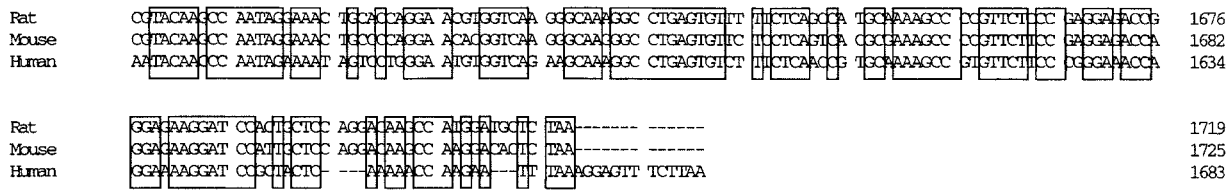

Fig. 3. (*Continued*)

protein of 572 amino acids with a predicted molecular weight of 63.8 kD.

Comparison of the sequence of rat osteoactivin with public databases revealed that it is highly homologous to the human (GenBank accession X7653) and mouse (GenBank accession AF322054 and AJ251685) *nmb* DNA and protein sequences. A comparison of the nucleotide sequences of the open reading frames (Fig. 3) and predicted protein sequences (Fig. 4) of rat osteoactivin with human *nmb* reveals a 77% identity on the DNA level (excluding the coding sequences for the 14 amino acid insertion in the predicted protein) and a 65% identity on the protein level. As can be seen in Figure 4, the predicted protein sequences of rat osteoactivin and mouse *nmb* have a proline-serine rich insertion of 14 or 16 amino acids, respectively, beginning at rat residue 329 that is not present in the human *nmb* sequence.

Since no data were previously available as to the function of osteoactivin or *nmb*, bioinformatic analysis of the osteoactivin protein sequence was performed. We used the CBS Signal P V1.1 World Wide Web Prediction Server at the Center for Biological Sequence (http://www.cbs.dtu.dk) to analyze the sequence of osteoactivin for the presence of a signal peptide. Signal P calculates the maximal C-(raw cleavage site score), S-(signal peptide score) and Y-(combined cleavage site score) scores, and the mean S-score, between the N-terminal and the predicted cleavage site. Signal P analysis of osteoactivin revealed a mean S score of 0.907 indicating that it has a signal peptide (Fig. 5, Table I). This signal peptide consists of the first 22 amino acids with a predicted cleavage site between residues 22 and 23 (Fig. 4, arrow and Fig. 5). These data suggest that osteoactivin is a secreted protein. Hydropathy analysis revealed the presence of

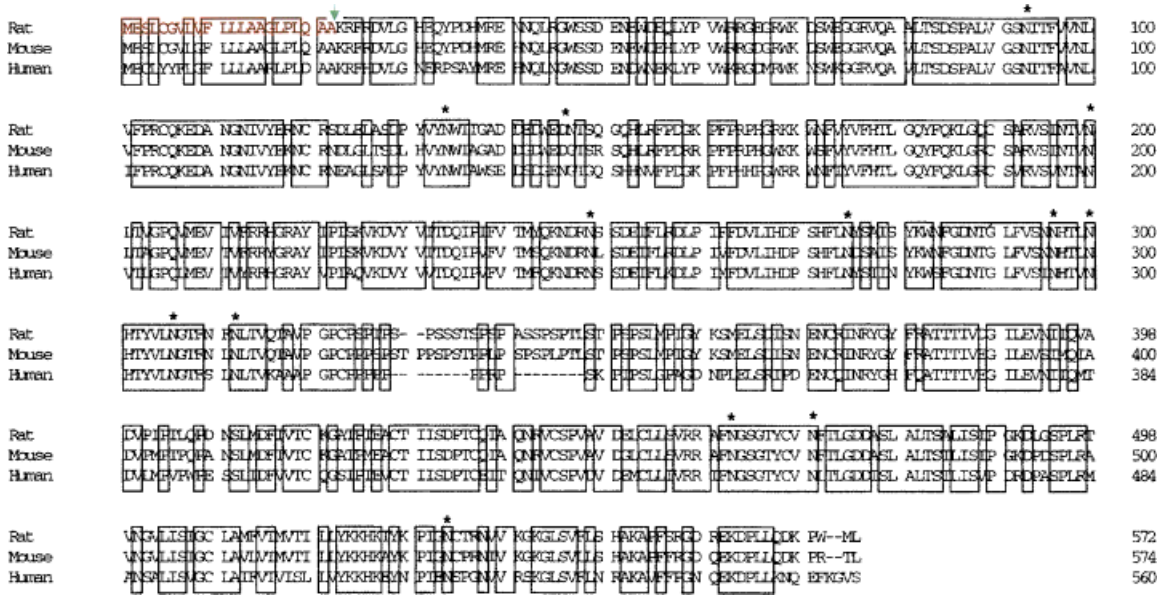

Fig. 4. Comparison of the predicted amino acid sequences of rat osteoactivin and mouse and human *nmb*. The predicted protein sequences of rat osteoactivin and mouse and human *nmb* are compared. Amino acid residues that are identical among the three species are boxed. The predicted rat osteoactivin and mouse *nmb* proteins have a proline-serine rich insertion beginning at residue 329 of the rat protein that is not present in the human *nmb* sequence. At the protein level, the sequences of rat osteoactivin and human *nmb* are 65% identical. The predicted rat osteoactivin protein contains a leader sequence with its cleavage site after residue 22 (arrow) as well as 13 potential sites for *N*-linked glycosylation (*). [Color figure can be viewed in the online issue, which is available at www.interscience.wiley.com.]

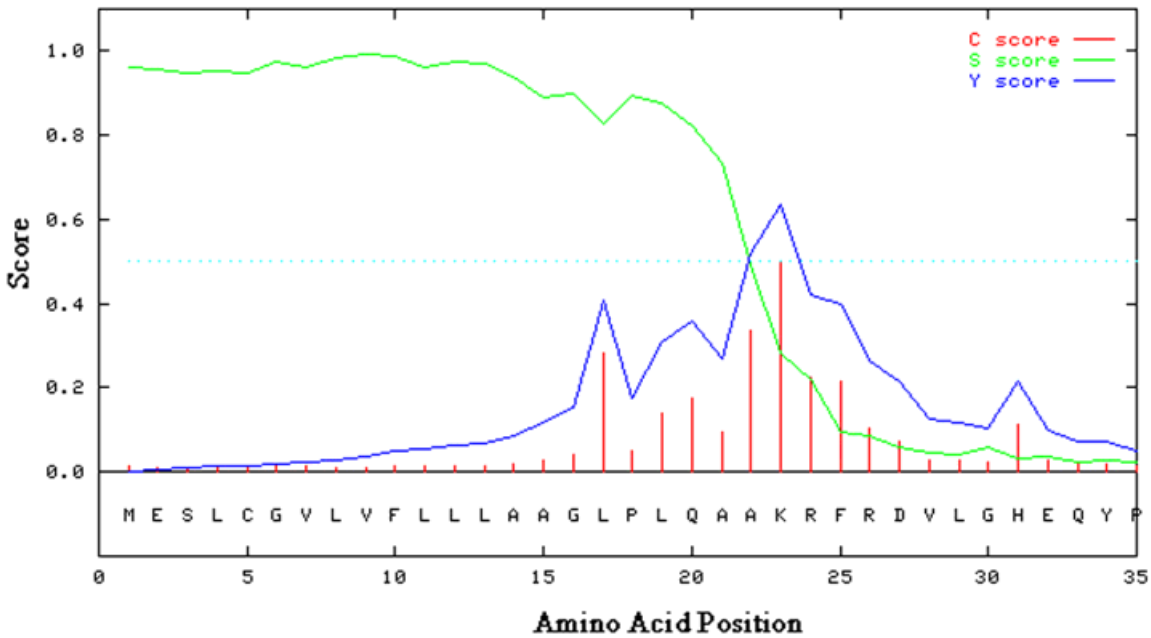

Fig. 5. Analysis of osteoactivin predicted amino acid sequence. Signal peptide prediction plot using the neural network model indicates a potential leader sequence at the amino terminus of osteoactivin. Mean S score = 0.907 which represents a signal peptide consisting of the first 22 amino acids and a cleavage site between position 22 and 23. [Color figure can be viewed in the online issue, which is available at www.interscience.wiley.com.]

several potential transmembrane spanning regions throughout the molecule as well as 13 sites of potential N-linked glycosylation consistent with the data reported for human *nmb* [Weterman et al., 1995] (data not shown). Osteoactivin also contains four sites for protein kinase C phosphorylation, 14 cysteine residues, and an RGD site located at position 556.

Expression of Osteoactivin in Other Tissues/Organs

To determine whether osteoactivin mRNA is expressed in other tissues/organs and to compare its relative levels of expression with bone, RT-PCR and Northern blot analyses were performed using total RNA isolated from various soft tissues and bone as well as from primary osteoblast cultures. The results of RT-PCR analysis demonstrated that osteoactivin mRNA is expressed at highest levels in long bones, calvaria and cultured osteoblasts, with much lower levels in thymus, brain and skeletal muscle (Fig. 6). Osteoactivin mRNA was not detectable in the other tissues examined including liver, heart, spleen, kidney, skin, proximal small intestine, and bone marrow (Fig. 6). These results were confirmed by Northern blot analysis although the sensitivity was lower making it difficult to detect distinct bands in the soft tissues with low levels of expression (data not shown).

In Situ Hybridization of Osteoactivin in Bone

Given the relatively high levels of osteoactivin expression in cultured rat osteoblasts, in situ hybridization was employed to localize the

TABLE I. Characterization of Predicted Osteoactivin Amino Acid Sequence

Amino Acid Position	Description
1–22	Signal peptide
23	Cleavage site
93, 134, 147, 200, 249, 275, 296, 300, 306, 312, 461, 469, 532	N-glycosylation site
191, 280, 417, 455, 526	Protein kinase C phosphorylation site
556	RGD site, cell attachment sequence
5, 105, 120, 190, 323, 371, 418, 427, 435, 443, 452, 467, 508, 533	Cysteine residues
166	Amidation site

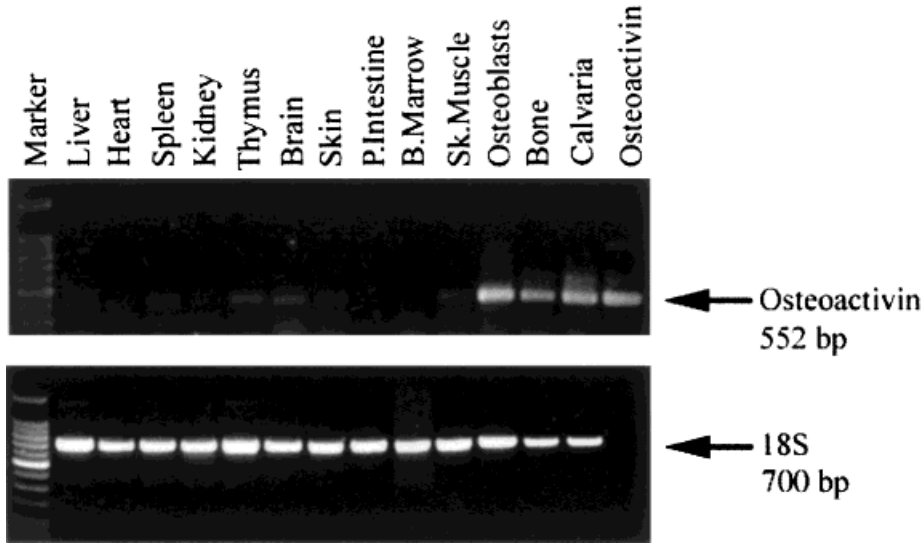

Fig. 6. PCR analysis of osteoactivin mRNA in multiple tissues. Total RNA was isolated from soft tissues, bone and osteoblast cultures, as described in the methods. Two micrograms of total RNA was reversed transcribed to generate first strand cDNA. The generated cDNAs from different tissues and osteoblast cultures were subjected to PCR using specific primers for osteoactivin and 18S as internal control. PCR products were separated on 1% agarose gel and stained with ethedium bromide. PCR product for osteoactivin was 552 bp and for 18S was 700 bp. cDNA for osteoactivin was used as an internal positive control. PCR was repeated three times using independent cDNA samples with similar results. Although low levels of osteoactivin expression were detected in thymus, brain, and skeletal muscle, maximum levels were detected in long bones, calvaria and primary osteoblast cultures.

expression of osteoactivin mRNA in cells within the bone microenvironment. Sections of the proximal tibial metaphysis from 2-week-old normal rats were prepared and hybridized to sense and anti-sense osteoactivin riboprobes. Using the anti-sense riboprobe, the detection signal for osteoactivin mRNA was predominantly located in rows of plump, cuboidal osteoblasts lining active bone forming surfaces (Fig. 7, arrows). Osteoactivin mRNA was also detected in some osteocytes, particularly those most recently encased in bone and close to the bone surface. In addition, a few cells scattered among the intertrabecular spaces of the metaphysis also exhibited signal for osteoactivin mRNA. These data demonstrate that osteoactivin is primarily expressed in osteoblasts.

Temporal Expression of Osteoactivin in Primary Osteoblast Cultures

Primary cultures of osteoblasts derived from calvarial digests of newborn normal rat calvaria were established and used to examine the expression of osteoactivin mRNA during osteoblast differentiation. In these cultures, there are three distinct stages of osteoblast development including an initial period of cell proliferation (from initiation to day 7), followed by a period of matrix formation and maturation (day 7–14), and ending with a final phase of matrix mineralization (day 14–21) [Owen et al., 1990]. For each experiment, cultures were established at the same time and terminated at various time points for RNA isolation. Northern blot analysis clearly shows a temporal pattern of expression for osteoactivin, which, although detectable at low levels in proliferating osteoblasts, progressively increases as the cells differentiate being highest during the period of matrix mineralization (Fig. 8). The pattern of osteoactivin expression in these cultures is very similar to that of alkaline phosphatase, a gene highly expressed during the periods of maturation and matrix mineralization. Peak expression of osteoactivin also correlates with the peak expression, at day 21, of osteocalcin, a marker for osteoblast terminal differentiation.

DISCUSSION

In the present study, we used mRNA differential display (DD) to compare the expression of genes in bone from osteopetrotic (*op*) and normal rats. This technique was initially described by Liang and Pardee [1992]; Liang et al. [1993] as a way to bring the remarkable

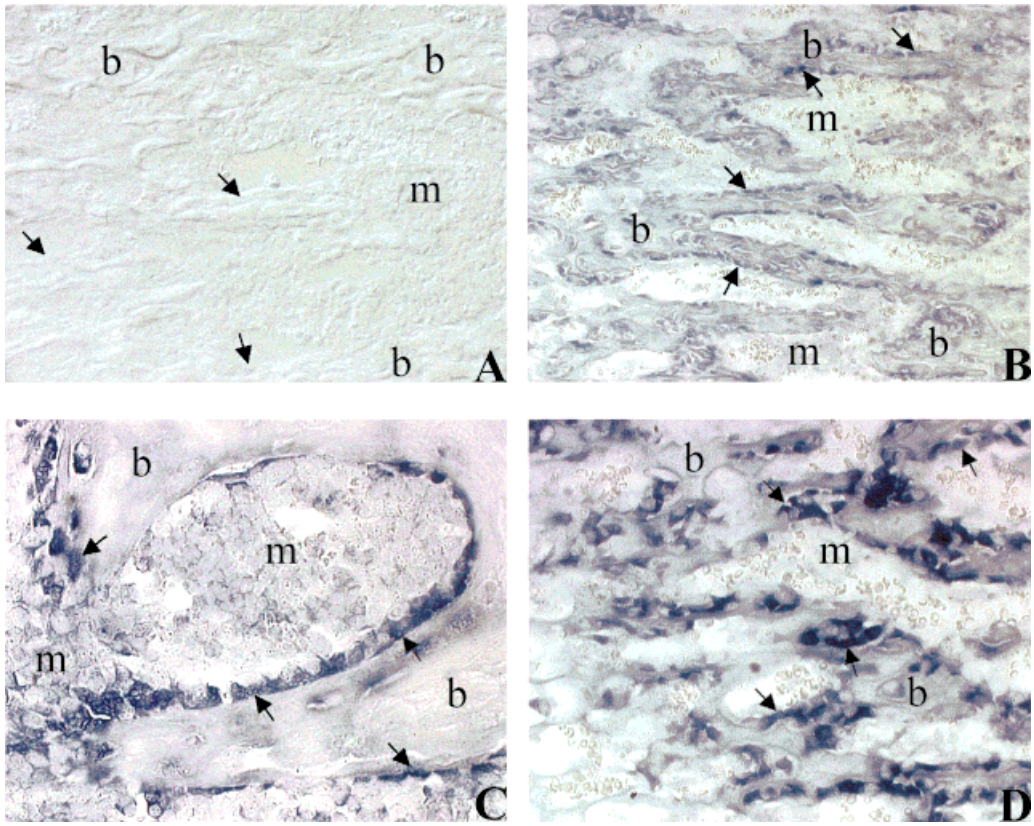

Fig. 7. In situ hybridization (ISH) of osteoactivin in bone. Sections of proximal tibial metaphyses of 2-week-old normal rats were processed for ISH as described in the methods. **A:** Sections incubated with the osteoactivin sense riboprobe were used as a control. Note the absence of any reaction product; image was captured using Nomarski DIC microscopy to allow visualization of some detail of the unstained tissue. **B–D:** Low, medium and high power photomicrographs of sections hybridized with the osteoactivin anti-sense riboprobe. Note the reaction product indicative of osteoactivin mRNA expression specifically associated with osteoblasts (arrows) lining the bony trabeculae (b), m: marrow spaces.

power and sensitivity of the polymerase chain reaction (PCR) to bear on questions of differences in gene expression. The advantages of DD include its lack of bias and high sensitivity. The absence of bias means that no prior assumptions need to be made as to the biological mechanisms and the method is capable of detecting novel gene products. The PCR-based sensitivity of DD also permits the detection of minor changes in gene expression. The main disadvantage of the method is that it is prone to producing false positives and this requires careful attention to experimental conditions and the use of appropriate controls. Most importantly, any differences observed by DD must be confirmed by Northern blot analysis.

Mason et al. [1997] utilized this approach to study bone cell gene expression and found that the glutamate signaling pathway is involved in the response of bone to mechanical loading. We used this technique to clone and characterize connective tissue growth factor (CTGF) that was highly overexpressed in *op* mutant compared to normal bone [Xu et al., 2000]. CTGF is a secreted, extracellular matrix-associated protein that was previously shown to be produced by various cell types including fibroblasts, endothelial cells, and chondrocytes [Lau and Lam, 1999]. CTGF has been shown to regulate diverse cellular functions including cell proliferation, attachment, migration, differentiation, survival and matrix production [Moussad and Brigstock, 2000]. Our studies demonstrated that CTGF is also produced by osteoblasts and appears to play an important role in regulating osteoblast differentiation and function (unpublished observations).

In this study, we identified a novel cDNA, named osteoactivin that was overexpressed in *op* mutant compared to normal bone. Confirmation by Northern blot analysis demonstrated that osteoactivin expression was increased 3- to 4-fold in *op* versus normal long bones and calvaria. Osteoactivin cDNA was cloned and

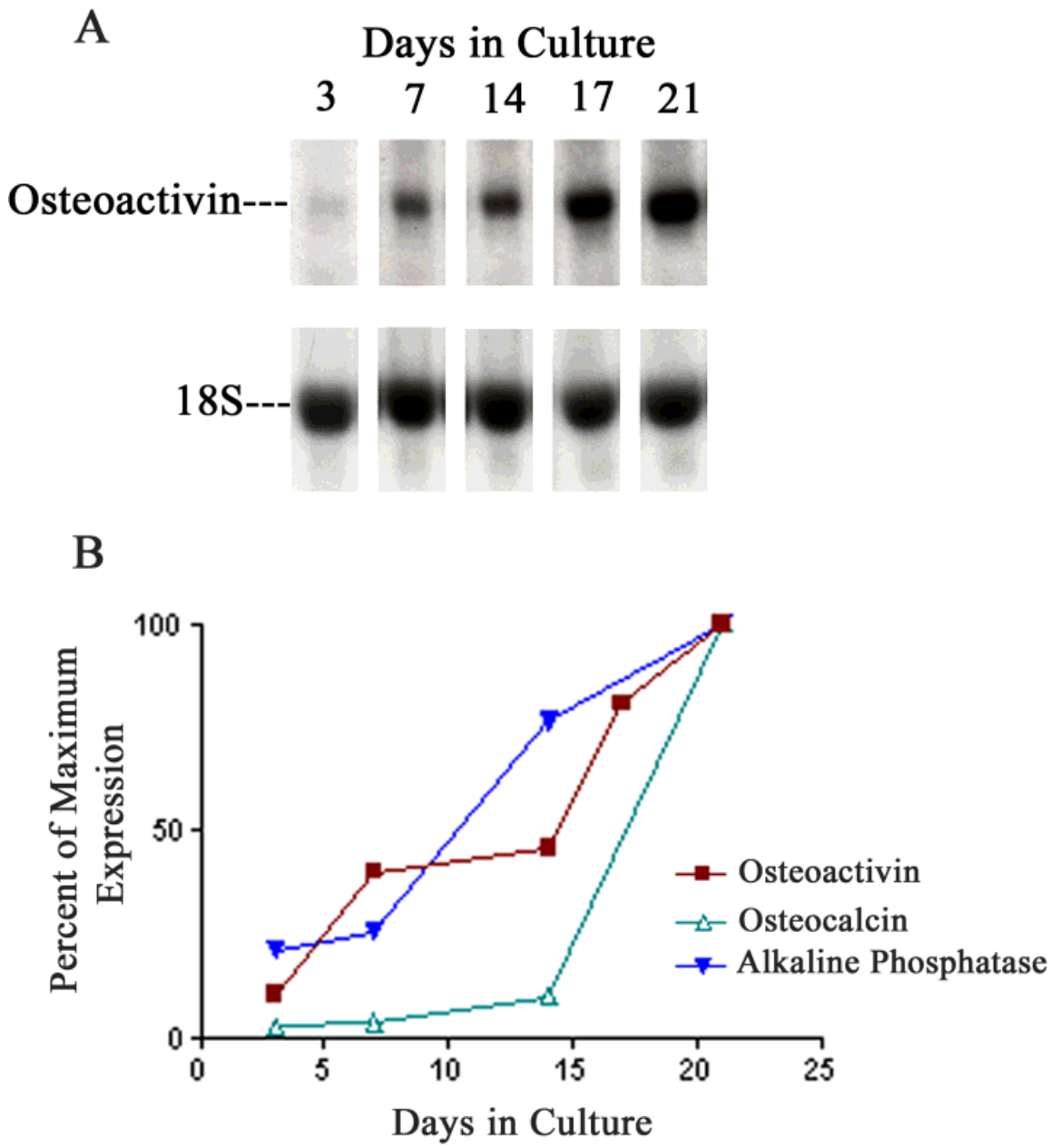

Fig. 8. Temporal expression of osteoactivin mRNA in primary rat osteoblast cultures. **A:** Twenty micrograms of total RNA isolated from osteoblasts cultured for 3, 7, 14, 17, and 21 days, was electrophoresed, blotted, and probed for osteoactivin. Blot was stripped and reprobed for alkaline phosphatase (AP), osteocalcin (OC) and, finally, 18S rRNA as a loading control. **B:** The results of three independent experiments were quantitated by scanning densitometry and plotted relative to the maximal expression of each transcript corrected using the 18S rRNA control. [Color figure can be viewed in the online issue, which is available at www.interscience.wiley.com.]

sequenced; it was found to have 77% identity on the DNA level and 65% identity of the protein level to human *nmb*. Human *nmb* was isolated by subtractive hybridization of MV1 and MV3 melanoma cell lines that exhibit low and high metastatic potential in nude mice, respectively; *nmb* was found to be overexpressed in MV1 when compared to MV3 cells [Weterman et al., 1995], although the function of *nmb* is unknown. Osteoactivin also shares sequence homology with *Pmel 17*, a melanocyte-specific gene that may function as a catalyst in melanin biosynthesis [Kwon et al., 1991]. Osteoactivin has an open reading frame (ORF) of 1,716 bp with a short 5′ untranslated region and encoding a protein of 572 amino acids with a predicted

molecular weight of 63.8 kD. Its sequence resembles that of *Pmel 17* which has an ORF that encodes a protein of 645 amino acids and a molecular weight of 68.6 kD. The first 22 amino acids of osteoactivin and the first 23 amino acids of *Pmel 17* represent potential signal peptides, characteristic of secreted proteins. These similarities suggest that osteoactivin may belong to the same gene family as *Pmel 17*.

Analysis of the predicted amino acid sequence for osteoactivin revealed 13 potential *N*-linked glycosylation sites and it is known that glycosylation of a protein can have a significant impact on its biological activity. Other features that are also likely to regulate its biological activity include the four sites for protein kinase C phosphorylation and 14 cysteine residues. An RGD site, located at position 556, represents a potential site for cell attachment and may be important for osteoactivin binding and its mechanism of action. Since there are no previous studies on osteoactivin and the function of human *nmb* is unknown, there is a great deal of work that needs to be done to determine the functions of osteoactivin and its mechanism(s) of action.

Tissue distribution of osteoactivin expression measured by RT-PCR analysis showed that osteoactivin is expressed at highest levels in bone and primary osteoblast cultures with lower levels of expression in brain, thymus, and skeletal muscle. Its high level of expression in developing bone suggests that it may play a role as a local regulator of bone cell metabolism. In situ hybridization was performed to localize osteoactivin mRNA expression in cells of the bone microenvironment. These experiments revealed that osteoactivin mRNA is primarily localized in plump, cuboidal osteoblasts lining bone surfaces.

These data led us to examine osteoactivin expression in primary osteoblast cultures derived from newborn rat calvaria. This culture system is routinely employed to examine the effects of local and systemic factors (e.g., hormones, cytokines, growth factors) on osteoblast development and function. Primary osteoblast cultures undergo three distinct stages beginning with cell proliferation (day 0–7) associated with the expression of histone H4, TGF-β and fibronectin, followed by a period of matrix maturation (day 7–14) associated with the expression of alkaline phosphatase and matrix Gla protein, and ending with a stage of matrix mineralization (day 14–21) associated with the expression of genes characteristic of the terminally differentiated osteoblast including osteocalcin and osteopontin [Stein et al., 1996]. In this study, we examined the temporal pattern of osteoactivin expression and showed that it increased progressively as the cells differentiated with maximum expression during the final stage of matrix mineralization. Osteoactivin expression was also correlated with the expression of the osteoblast-related genes alkaline phosphatase and osteocalcin in these cultures. The data suggest that osteoactivin may play an important role in osteoblast differentiation and matrix mineralization. Clearly, additional studies are necessary to determine whether it is secreted in culture and to examine its functional role. Experiments to block its expression using an anti-sense oligonucleotide and/or a neutralizing antibody are planned and expected to shed some light on the functional properties of this novel protein.

The overexpression of osteoactivin in *op* mutant compared to normal bone is an interesting finding that also requires further investigation. The rat mutation, *osteopetrosis* (*op*) mutation is among a group of spontaneous, autosomal recessive mutations in rodents that exhibit the characteristic feature of generalized skeletal sclerosis [Seifert et al., 1993]. Characterization of *op* bone has revealed that osteoclasts are present but exhibit atypical morphological features, suggesting that the defect involves cell function instead of development [Marks and Popoff, 1989]. Furthermore, the ability of normal bone marrow transplantation to restore osteoclastic bone resorption and cure the skeletal manifestations provides direct evidence that the defect is inherent to cells of the osteoclast lineage [Popoff et al., 1994]. Despite the fact that the *op* rat mutation is caused by a primary defect in osteoclast-mediated bone resorption, abnormalities involving osteoblast gene expression have been reported. The expression of some osteoblast-related genes are markedly increased in *op* versus normal bone [Shalhoub et al., 1991]. Therefore, it is perhaps not surprising that osteoactivin, another osteoblast-related gene, is also upregulated in *op* bone. These abnormalities are likely to be secondary to the absence of normal osteoclast function causing an uncoupling of bone resorption from bone formation. The resulting dysregulation of osteoblast gene

expression and function would be consistent with our findings, although the factor(s) that drive this overexpression are unknown. Future studies will focus on systemic and local factors known to be upregulated in the *op* mutation, such as $1,25(OH)_2D_3$, PTH, TGF-β, c-*fos* and others, and are expected to shed light on transcriptional regulation of osteoactivin as well as provide an explanation for its upregulation in *op* bone.

ACKNOWLEDGMENTS

The authors would like to thank members of the DNA sequencing facility at Pfizer Global Research and Development for performing the sequencing for this project. The authors would also like to thank Dr. Victoriya Zakhaleva for her technical assistance and Cherie Glanzmann for her assistance in preparing the manuscript. This study was supported by a research grant from Pfizer, Inc. (to S.N.P. and F.F.S.) and by funds awarded to the Bone Research Enterprise Program by Temple University School of Medicine.

REFERENCES

Beck GR Jr, Zerler B, Moran E. 2001. Gene array analysis of osteoblast differentiation. Cell Growth Differ 12:61–83.

Grewal TS, Genever PG, Brabbs AC, Birch M, Skerry TM. 2000. Best5: a novel interferon-inducible gene expressed during bone formation. FASEB J 14(3):523–531.

Guide for the care and use of laboratory animals. 1985. U.S. Dept. of Health and Human Services, National Institutes of Health Publ. No. 86-23.

Hermey DC, Ireland RA, Zerwekh JE, Popoff SN. 1995. Regulation of mineral homeostasis in osteopetrotic (op) rats. Am J Physiol 268:E312–E317.

Horowitz MC, Xi Y, Wilson K, Kacena MA. 2001. Control of osteoclastogenesis and bone resorption by members of the TNF family of receptors and ligands. Cytokine Growth Factor Rev 12(1):9–18.

Kwon BS, Chintamaneni C, Kozak CA, Copeland NG, Gilbert DJ, Jenkins N, Barton D, Francke U, Kobayashi Y, Kim KK. 1991. A melanocyte-specific gene, *Pmel 17*, maps near the silver coat color locus on mouse chromosome 10 and is in a syntenic region on human chromosome 12. Prac Natl Acad Sci 88:9228–9232.

Lau LF, Lam SCT. 1999. The CCN family of angiogenic regulators: the integrin connection. Exper Cell Res 248: 44–57.

Liang P, Pardee AB. 1992. Differential display of eukaryotic messenger RNA by means of the polymerase chain reaction. Science 257:967–971.

Liang P, Averboukh L, Pardee AB. 1993. Distribution and cloning of eukaryotic mRNAs by means of differential display: refinements and optimization. Nucleic Acids Res 21:3269–3275.

Marks SC Jr, Hermey DC. 1996. The structure and development of bone. In: Bilezikian JP, Raisz LG, Rodan GA, editors. Principles of bone biology. San Diego: Academic Press. p 69–85.

Marks SC Jr, Popoff SN. 1989. Osteoclast biology in the osteopetrotic (*op*) rat. Am J Anat 186:325–334.

Mason DJ, Suva LJ, Genever PG, Patton AJ, Steuckle S, Hillam RA, Skerry TM. 1997. Mechanically regulated expression of a neural glutamate transporter in bone: a role for excitatory amino acids as osteotropic agents? Bone 20:199–205.

Moussad EEA, Brigstock DR. 2000. Connective tissue growth factor: what's in a name? Molec Genet Metab 71:276–292.

Owen TA, Aronow M, Shalhoub V, Barone LM, Wilming L, Tassinari MS, Kennedy MB, Pockwinse S, Lian JB, Stein GS. 1990. Progressive development of the rat osteoblast phenotype in vitro: reciprocal relationships in expression of genes associated with osteoblast proliferation and differentiation during formation of the bone extracellular matrix. J Cell Physiol 143:420–430.

Petersen DN, Tkalcevic GT, Mansolf AL, Rivera-Gonzalez R, Brown TA. 2000. Identification of osteoblast/osteocyte 45 (OF45), a bone-specific cDNA encoding an RGD-containing protein that is highly expressed in osteoblasts and osteocytes. J Biol Chem 275(46):36172–36180.

Popoff SN, Marks SC Jr. 1995. The heterogeneity of the osteopetroses reflects the diversity of cellular influences during skeletal development. Bone 17:437–445.

Popoff SN, Schneider GB. 1996. Animal models of osteopetrosis: the impact of recent molecular developments on novel strategies for therapeutic intervention. Mol Med Today 2:349–358.

Popoff SN, Osier LK, Zerwekh JE, Marks SC Jr. 1994. Interdependence of skeletal sclerosis and elevated circulating levels of 1.25-dihydroxyvitamin D in osteopetrotic (*op* and *tl*) rats. Bone 15:515–522.

Popoff SN, Xu J, Smock S, Mendis M, Zakhaleva V, Owen TA, Safadi FF. 2000. Regulation of connective tissue growth factor in primary rat osteoblast cultures by $1,25(OH)_2D_3$. In Vitamin D Endocrine System: Structural, Biological, Genetic and Clinical Aspects. Hawthorne, NY: Walter de Gruyer. p 192–132.

Ryoo HM, van Wijnen AJ, Stein JL, Lian JB, Stein GS. 1997. Detection of a proliferation specific gene during development of the osteoblast phenotype by mRNA differential display. J Cell Biochem 64(1):106–116.

Safadi FF, Seifert MF, Popoff SN. 1999. Skeletal resistance to 1,25-dihydroxyvitamin D_3 in osteopetrotic rats. Endocrine 11:309–319.

Seifert MF, Popoff SN, Jackson ME, MacKay CA, Cielinski M, Marks SC Jr. 1993. Experimental studies of osteopetrosis in laboratory animals. Clin Orthopaed 294:23–33.

Seth A, Lee BK, Qi S, Vary CP. 2000. Coordinate expression of novel genes during osteoblast differentiation. J Bone Miner Res 15(9):1683–1696.

Shalhoub V, Jackson ME, Lian JB, Stein GS, Marks SC Jr. 1991. Gene expression during skeletal development in three osteopetrotic rat mutations. J Biol Chem 266: 9847–9856.

Stein GS, Lian JB, Stein JL, van Wijnen AJ, Frennkel B, Montecino M. 1996. Mechanisms Regulating osteoblast proliferation and differentiation. In: Bilezikian JP,

Raisz LG, Rodan GA, editors. Principles of bone biology. San Diego: Academic Press. p. 69–85.

Teitelbaum SL. 2000. Bone resorption by osteoclasts. Science 289:1504–1508.

Thiede MA, Smock SL, Petersen DN, Grasser WA, Thompson DD, Nishimoto SK. 1994. Presence of messenger ribonucleic acid encoding osteocalcin, a marker of bone turnover, in bone marrow megakaryocytes and peripheral blood platelets. Endocrinology 135:929–937.

Triffitt JT. 1996. The stem cell of the osteoblast. In: Gold L, Cleveland D, editors. Oral and maxillofacial surgery clinics of North America. Philadelphia: WB Saunders. p 39–50.

Weterman MA, Ajubi N, van Dinter IM, Degen WG, van Muijen GN, Ruitter DJ, Bloemers HP. 1995. nmb, a novel gene, is expressed in low-metastatic human melanoma cell lines and xenografts. Int J Cancer 60(1):73–81.

Xu J, Smock SL, Safadi FF, Rosenzweig AB, Odgren PR, Marks SC Jr, Owen TA, Popoff SN. 2000. Cloning the full-length cDNA for rat connective tissue growth factor: implications for skeletal development. J Cell Biochem 77:103–115.

Yamamoto N, Lindsay DD, Naraparaju VR, Ireland RA, Popoff SN. 1994. A defect in the inflammation-primed macrophage-activation cascade in osteopetrotic rats. J Immunol 152(10):5100–5107.

Zhou H, Kartsogiannis V, Hu YS, Elliott J, Quinn JM, McKinstry WJ, Gillespie MT, Ng KW. 2001. A novel osteoblast-derived c-type lectin that inhibits osteoclast formation. J Biol Chem 276(18):14916–14923.